

# Multiatom and resonant interaction scheme for quantum state transfer and logical gates between two remote cavities via an optical fiber

Zhang-qi Yin and Fu-li Li\*

*Department of Applied Physics, Xi'an Jiaotong University, Xi'an 710049, China*

## Abstract

A system consisting of two single-mode cavities spatially separated and connected by an optical fiber and multiple two-level atoms trapped in the cavities is considered. If the atoms resonantly and collectively interact with the local cavity fields but there is no direct interaction between the atoms, we show that an ideal quantum state transfer and highly reliable quantum swap, entangling, and controlled-Z gates can be deterministically realized between the distant cavities. We find that the operation of state transfer and swap, entangling, and controlled-Z gates can be greatly speeded up as number of the atoms in the cavities increases. We also notice that the effects of spontaneous emission of atoms and photon leakage out of cavity on the quantum processes can also be greatly diminished in the multiatom case.

PACS numbers: 03.67.Lx, 03.67.Mn, 42.81.Qb

---

\*Email: flli@mail.xjtu.edu.cn

## I. INTRODUCTION

Quantum computers implement computational tasks on the basis of the fundamental quantum principle. Shor [1] showed that a quantum computer could complete the factorization of large composite numbers into primes in only polynomial time, which is the basis of the security of many classical key cryptosystems. Grover [2] discovered a quantum algorithm that searches a number from a disordered database polynomially faster than any classical algorithms. The progress has greatly stimulated much interest in quantum computer and quantum computation.

For building a quantum computer that could be used to solve some practical problems, a large number of qubits such as either trapped atoms or ions must be assembled together and manipulated according to certain orders [3]. In order to work in this way, *distributed quantum computing* is introduced [4]. Distributed quantum computing is an architecture in which a quantum computer is thought as a network of spatially separated local processors that contain only a few qubits and are connected via quantum transmission lines [5]. One of the key problems in the realization of distributed quantum computing is how to implement two-qubit quantum gates among local processors since a quantum computer can be built by assembling two-quantum-bit logic gates [6, 7]. Controlled-phase gates between atoms trapped in distant optical cavities have been recently proposed [8, 9, 10, 11, 12]. Several schemes which are based on cavity QED systems have also been proposed to implement quantum communication or engineer entanglement between atoms trapped in two distant optical cavities [13, 14, 15, 16, 17, 18, 19]. In some of these schemes [13, 14, 15, 16], two spatially separated cavities are directly connected to each another via quantum channels. In order to realize quantum logical gates, accurately tailored sequences of controlling pulses or adiabatic processes are involved and considerable local operations are required. In other schemes [17, 18, 19], the detection of leaking photons is involved. The quantum logical gates are realized only in a probabilistic way and the success probability is highly dependent on the efficiency of photon detectors. Therefore, it is highly desired that deterministic quantum gates between two separated subsystems can be implemented in coherent evolutions of the entire system. In the recent paper [20], Serafini et al. investigated the possibility of realizing deterministic swap and controlled-phase gates between two-level atoms trapped in separate optical cavities, through a coherent resonant coupling mediated by an optical fiber. In the

scheme, each of the cavities contains a single two-level atom, and the only local control required is the synchronized switching on and off of the atom-field interaction in the distant cavities, achievable through simple control pulses.

In practical situations, various decoherence processes such as spontaneous emission of atoms and photon leakage out of cavities are inevitable. In order to diminish the effects of dissipation processes on quantum information processing, the operation time of quantum gates must be much shorter than the characteristic time of various relaxations. In the present study, we consider the scheme, similar to that proposed by Serafini et al. [20], however, multi two-level atoms are trapped in each of the cavities and a qubit is encoded in zero- and single-excitation Dicke states of the atoms. We find that perfect quantum-state transfer, and quantum swap, entangling and controlled-Z gates between the qubits can be realized, and moreover the operation time of these quantum processes is proportional to  $1/\sqrt{N}$  where  $N$  is number of the atoms trapped in each of the cavities. Therefore, the quantum processes under consideration can be greatly speeded up and the effects of spontaneous emission and photon leakage can be depressed if the number of atoms is large. We also find that highly reliable controlled-Z gate can be realized in the resonant interaction with much shorter operation time than that in the non-resonant case which was considered in [20].

The paper is organized as follows. In section II, we introduce the model under consideration. In Sections III, IV, V and VI, quantum state transfer, and swap, entangling and controlled-Z gates are investigated, respectively. In Section VII, the influence of atomic spontaneous emission and photon leakage out of the cavities and fiber on the quantum state transfer, and the swap, entangling and controlled-Z gates is investigated. In section VIII, a summary is given.

## II. MODEL

As shown in Fig. 1, multi two-level atoms are trapped in two distant single-mode optical cavities, which are connected by an optical fiber. The atoms resonantly interact with the local cavity fields. We assume that the size of the space occupied by the atoms in each of the cavities is much smaller than the wavelength of the cavity field. Then, all the atoms in each of cavities “see” the same field. On the other hand, the atoms in the same cavity are so separated that they have no direct interaction each other. The collectively raising and

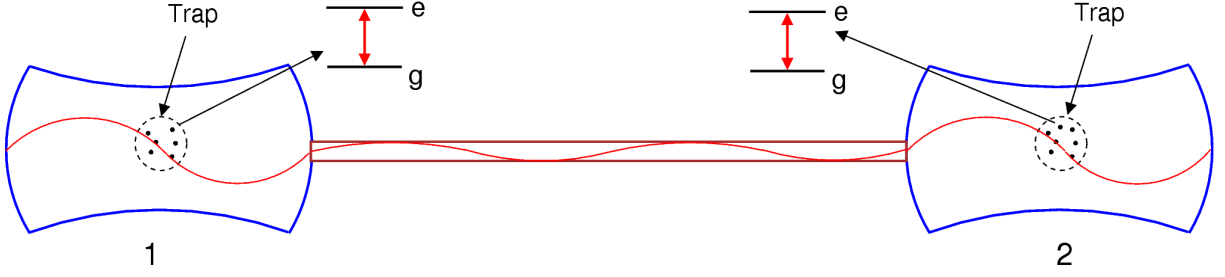


FIG. 1. Experimental setup.

lowering operators for the atoms in cavity  $j(=1,2)$  are defined as

$$J_j^\pm = \sum_{i=1}^{N_j} \sigma_i^\pm(j), \quad (1)$$

where  $N_j$  is the number of atoms in cavity  $j$ ,  $\sigma_i^-(j) = |g_i\rangle\langle e_i|$  and  $\sigma_i^+(j) = (\sigma_i^-)^\dagger$  for atom  $i$  in cavity  $j$  with the ground state  $|g\rangle$  and the excited state  $|e\rangle$ . In rotating wave approximation, the interaction Hamiltonian of the atom-field system can be written as

$$H_{AF} = \sum_{j=1}^2 \left( g_j J_j^- a_j^\dagger + \text{h.c.} \right), \quad (2)$$

where  $a_j^\dagger$  is the creation operator for photons in the mode of cavity  $j$ , and  $g_j$  is the coupling constant between the mode of cavity  $j$  and the trapped atoms.

The coupling between the cavity fields and the fiber modes may be modeled by the interaction Hamiltonian [14]

$$H_{IF} = \sum_{j=1}^{\infty} \nu_j \left[ b_j (a_1^\dagger + (-1)^j e^{i\varphi} a_2^\dagger) + \text{h.c.} \right], \quad (3)$$

where  $b_j$  is the creation operator for photons in mode  $j$  of the fiber,  $\nu_j$  is the coupling strength with fiber mode  $j$ , and the phase  $\varphi$  is induced by the propagation of the field through the fiber of length  $l$ :  $\varphi = 2\pi\omega l/c$ . The Hamiltonian  $H_{IF}$  holds for high finesse cavities and resonant operations over the time scale much longer than the fiber's round-trip time [15]. In the short fiber limit  $(2L\bar{\nu})/(2\pi C) \leq 1$ , where  $L$  is the length of fiber and  $\bar{\nu}$  is the decay rate of the cavity fields into a continuum of fiber modes, only one resonant mode  $b$  of the fiber interacts with the cavity modes. Therefore, for this case, the Hamiltonian  $H_{IF}$  may be approximated to [20]

$$H_{IF} = \nu \left[ b(a_1^\dagger + a_2^\dagger) + \text{h.c.} \right], \quad (4)$$

where the phase  $\varphi$  has been absorbed into the annihilation and creation operators of the mode of the second cavity field.

In the interaction picture, the total Hamiltonian of the atom-cavity-fiber combined system is

$$H = \sum_{j=1}^2 \left( g_j J_j^- a_j^\dagger + \text{h.c.} \right) + \nu \left[ b(a_1^\dagger + a_2^\dagger) + \text{h.c.} \right]. \quad (5)$$

We introduce the total excitation operator  $\mathcal{N} = N_{1+} + N_{2+} + a_1^\dagger a_1 + a_2^\dagger a_2 + b^\dagger b$ , where  $N_{j+}$  is the number operator of atoms in the excited state in cavity  $j$ . It is easily shown that the excitation operator commutes with the Hamiltonian (5). Therefore, the total excitation number is a conserved quantity [21].

### III. QUANTUM STATE TRANSFER

We consider that  $N$  two-level atoms are trapped in each of the cavities and take the state  $|0, N\rangle$  where  $N$  atoms are all in the ground state as the computational basis  $|0\rangle$  and  $|1, N-1\rangle$  where  $N-1$  atoms are in the ground state and one atom in the excited state as the computational basis  $|1\rangle$ . Suppose that at the initial time all modes of both the cavities and fiber are not excited, and all the atoms in the first cavity are in a general superposition state of the two basis vectors  $\alpha|0, N\rangle_1 + \beta|1, N-1\rangle_1$ , where  $\alpha$  and  $\beta$  are complex numbers and are constrained only by the normalization condition, but all the atoms in the second cavity are in the state  $|0, N\rangle_2$ . The goal of quantum state transfer is to deterministically accomplish the operation:

$$(\alpha|0, N\rangle_1 + \beta|1, N-1\rangle_1) \otimes |0, N\rangle_2 \rightarrow |0, N\rangle_1 \otimes (\alpha|0, N\rangle_2 + \beta|1, N-1\rangle_2). \quad (6)$$

The time evolution of the total system is governed by the Schrödinger equation ( $\hbar = 1$ )

$$i \frac{\partial}{\partial t} |\Psi(t)\rangle = H |\Psi(t)\rangle. \quad (7)$$

Suppose that both the cavity and fiber fields are initially in the vacuum state  $|000\rangle_f$ . At time  $t$ , the system is in the state  $U(t)|000\rangle_f \otimes (\alpha|0, N\rangle_1 + \beta|1, N-1\rangle_1) \otimes |0, N\rangle_2 = \alpha|000\rangle_f \otimes |0, N\rangle_1 \otimes |0, N\rangle_2 + \beta U(t)|000\rangle_f \otimes |1, N-1\rangle_1 \otimes |0, N\rangle_2$ , where  $U(t) = \exp(-itH)$ . The state  $|000\rangle_f \otimes |1, N-1\rangle_1 \otimes |0, N\rangle_2$  belongs to the subspace with one excitation number, which is

spanned by the basis state vectors

$$\begin{aligned}
|\phi_1\rangle &= |000\rangle_f |0, N\rangle_1 |1, N-1\rangle_2, \\
|\phi_2\rangle &= |000\rangle_f |1, N-1\rangle_1 |0, N\rangle_2, \\
|\phi_3\rangle &= |001\rangle_f |0, N\rangle_1 |0, N\rangle_2, \\
|\phi_4\rangle &= |010\rangle_f |0, N\rangle_1 |0, N\rangle_2, \\
|\phi_5\rangle &= |100\rangle_f |0, N\rangle_1 |0, N\rangle_2,
\end{aligned} \tag{8}$$

where  $|n_1 n_f n_2\rangle_f$  denotes the field state with  $n_1$  photons in the mode of cavity 1,  $n_2$  in the mode of cavity 2 and  $n_f$  in the fiber mode, and  $|N_{j+}, N - N_{j+}\rangle_j$  is the state of atoms in cavity  $j$ , in which  $N_{j+}$  atoms are in the excited state and  $N - N_{j+}$  atoms in the ground state. A state of the entire system with one excitation number can be expanded in terms of the basis vectors (8) as

$$|\Psi(t)\rangle = \sum_{i=1}^5 C_i(t) |\phi_i\rangle. \tag{9}$$

Upon substitution of (9) in (7), Eq. (7) has the matrix form

$$i \frac{\partial}{\partial t} C_i(t) = \sum_{j=1}^5 H_{ij} C_j(t), \tag{10}$$

where  $H_{ij}$  are elements of the matrix representation for the Hamiltonian (5) in the one-excitation number subspace, i.e.,

$$H = \begin{pmatrix} 0 & 0 & \sqrt{N}g & 0 & 0 \\ 0 & 0 & 0 & 0 & \sqrt{N}g \\ \sqrt{N}g & 0 & 0 & \nu & 0 \\ 0 & 0 & \nu & 0 & \nu \\ 0 & \sqrt{N}g & 0 & \nu & 0 \end{pmatrix}, \tag{11}$$

where  $g_1 = g_2 = g$  has been assumed.

The Hamiltonian matrix (11) has five eigenvalues:  $E_1 = 0, E_{2,3} = \mp \sqrt{N}g, E_{4,5} =$

$\mp\sqrt{Ng^2 + 2\nu^2}$ . The corresponding eigenvectors are

$$\begin{aligned}
|\varphi_1\rangle &= -\frac{r}{\sqrt{1+2r^2}}|\phi_1\rangle - \frac{r}{\sqrt{1+2r^2}}|\phi_2\rangle + \frac{1}{\sqrt{1+2r^2}}|\phi_4\rangle, \\
|\varphi_2\rangle &= \frac{1}{2}|\phi_1\rangle - \frac{1}{2}|\phi_2\rangle - \frac{1}{2}|\phi_3\rangle + \frac{1}{2}|\phi_5\rangle, \\
|\varphi_3\rangle &= -\frac{1}{2}|\phi_1\rangle + \frac{1}{2}|\phi_2\rangle - \frac{1}{2}|\phi_3\rangle + \frac{1}{2}|\phi_5\rangle, \\
|\varphi_4\rangle &= -\frac{1}{2\sqrt{1+2r^2}}|\phi_1\rangle - \frac{1}{2\sqrt{1+2r^2}}|\phi_2\rangle + \frac{1}{2}|\phi_3\rangle - \frac{r}{\sqrt{1+2r^2}}|\phi_4\rangle + \frac{1}{2}|\phi_5\rangle, \\
|\varphi_5\rangle &= \frac{1}{2\sqrt{1+2r^2}}|\phi_1\rangle + \frac{1}{2\sqrt{1+2r^2}}|\phi_2\rangle + \frac{1}{2}|\phi_3\rangle + \frac{r}{\sqrt{1+2r^2}}|\phi_4\rangle + \frac{1}{2}|\phi_5\rangle,
\end{aligned} \tag{12}$$

where  $r = \nu/(\sqrt{N}g)$ . From (12), we deduce the unitary matrix  $S$  that diagonalizes the Hamiltonian matrix (11)

$$S = \begin{pmatrix} -\frac{r}{\sqrt{1+2r^2}} & -\frac{r}{\sqrt{1+2r^2}} & 0 & \frac{1}{\sqrt{1+2r^2}} & 0 \\ \frac{1}{2} & -\frac{1}{2} & -\frac{1}{2} & 0 & \frac{1}{2} \\ -\frac{1}{2} & \frac{1}{2} & -\frac{1}{2} & 0 & \frac{1}{2} \\ -\frac{1}{2\sqrt{1+2r^2}} & -\frac{1}{2\sqrt{1+2r^2}} & \frac{1}{2} & -\frac{r}{\sqrt{1+2r^2}} & \frac{1}{2} \\ \frac{1}{2\sqrt{1+2r^2}} & \frac{1}{2\sqrt{1+2r^2}} & \frac{1}{2} & \frac{r}{\sqrt{1+2r^2}} & \frac{1}{2} \end{pmatrix}. \tag{13}$$

By use of the unitary matrix  $S$ , Eq. (10) can be rewritten as the compact form

$$i\frac{\partial}{\partial t}SC = SHS^{-1}SC, \tag{14}$$

where  $C = [C_1, C_2, C_3, C_4, C_5]^T$ . Since the matrix  $SHS^{-1}$  is diagonal, a general solution of Eq. (10) is given by

$$C_j(t) = \sum_{k=1}^5 [S^{-1}]_{jk} [SC(0)]_k e^{-iE_k t}. \tag{15}$$

Using this solution, for the initial condition  $C(0) = [0, 1, 0, 0, 0]^T$ , we have

$$\begin{aligned}
|\Psi(t)\rangle &= U(t)|000\rangle_f \otimes |1, N-1\rangle_1 \otimes |0, N\rangle_2 \\
&= \left[ \frac{r^2}{1+2r^2} - \frac{1}{2} \cos(\sqrt{N}gt) + \frac{\cos(\sqrt{1+2r^2}\sqrt{N}gt)}{2(1+2r^2)} \right] |\phi_1\rangle \\
&+ \left[ \frac{r^2}{1+2r^2} + \frac{1}{2} \cos(\sqrt{N}gt) + \frac{\cos(\sqrt{1+2r^2}\sqrt{N}gt)}{2(1+2r^2)} \right] |\phi_2\rangle \\
&+ \left[ -\frac{i}{2} \sin(\sqrt{N}gt) + \frac{i \sin(\sqrt{1+2r^2}\sqrt{N}gt)}{2\sqrt{1+2r^2}} \right] |\phi_3\rangle \\
&+ \left[ -\frac{r}{1+2r^2} + \frac{r \cos(\sqrt{1+2r^2}\sqrt{N}gt)}{1+2r^2} \right] |\phi_4\rangle \\
&+ \left[ \frac{i}{2} \sin(\sqrt{N}gt) + \frac{i \sin(\sqrt{1+2r^2}\sqrt{N}gt)}{2\sqrt{1+2r^2}} \right] |\phi_5\rangle.
\end{aligned} \tag{16}$$

From (16), it is easily shown that at  $t = \pi/(\sqrt{N}g)$  the initial state  $|000\rangle_f \otimes |1, N-1\rangle_1 |0, N\rangle_2$  evolves in the state  $|000\rangle_f \otimes |0, N\rangle_1 |1, N-1\rangle_2$  if the parameter  $r$  fulfills the condition

$$r^2 = (4k^2 - 1)/2, \quad k = 1, 2, 3, \dots \quad (17)$$

Combining the above results together, we have  $U(\pi/\sqrt{N}g)|000\rangle_f \otimes (\alpha|0, N\rangle_1 + \beta|1, N-1\rangle_1) \otimes |0, N\rangle_2 = \alpha|000\rangle_f \otimes |0, N\rangle_1 \otimes |0, N\rangle_2 + \beta|000\rangle_f \otimes |0, N\rangle_1 \otimes |1, N-1\rangle_2$ . Therefore, the perfect quantum state transfer (6) is deterministically implemented. It is noticed that the operation time of the state transfer is  $\pi/(\sqrt{N}g)$ . So, the transfer process can be greatly speeded up with the large number of atoms even if the coherent interaction strength  $g$  is small.

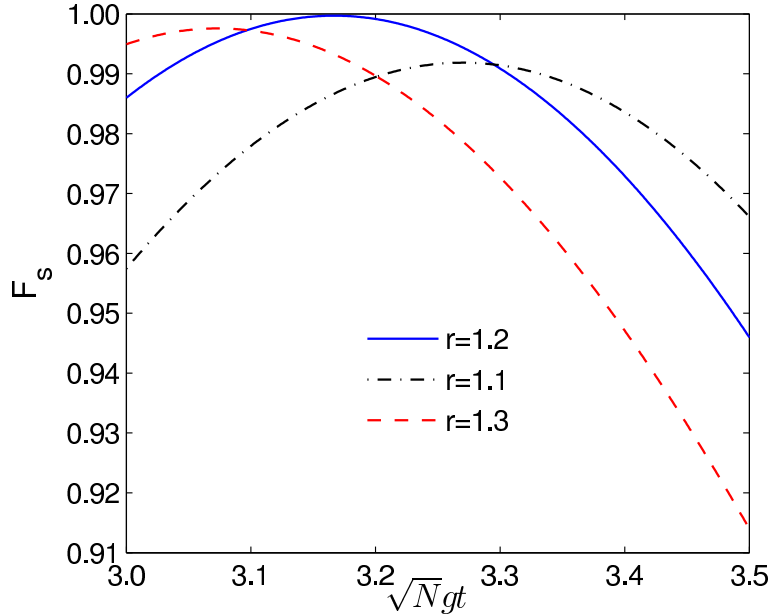


FIG. 2. Fidelity of the quantum state transfer as a function of  $\sqrt{N}gt$ .

If the condition (17) is strictly satisfied by the coupling constants, the ideal quantum state transfer can be implemented. In practical situations, however, the mismatch between the coupling strengths from the condition (17) inevitably happens. From (6), the target state of the transmission is  $|\psi_s\rangle = |000\rangle_f \otimes |0, N\rangle_1 \otimes (\alpha|0, N\rangle_2 + \beta|1, N-1\rangle_2)$ . Fidelity of the quantum state transfer is defined as  $F_s = |\langle\Psi(t)|\psi_s\rangle|^2$ . In Fig. 2, the fidelity is shown for the state transfer  $(|0, N\rangle_1 + |1, N-1\rangle_1)/\sqrt{2} \otimes |0, N\rangle_2 \rightarrow |0, N\rangle_1 \otimes (|0, N\rangle_2 + |1, N-1\rangle_2)/\sqrt{2}$  with different values of the parameter  $r$  around  $\sqrt{1.5}$  with which the perfect state transfer is implemented. One can observe that the fidelity is highly stable to the mismatch of the

coupling strengths from the condition (17). In Fig. 2, one may also observe that the fidelity varies smoothly as a function of the dimensionless time. This feature is useful for switching off the interaction between the atoms and the fields with control pulses once the quantum state transfer is achieved.

#### IV. QUANTUM SWAP GATE

Suppose that at the initial time all the atoms in cavity  $j$  are in a general superposition state:  $\alpha_j|0, N\rangle_j + \beta_j|1, N-1\rangle_j$  and all modes of both the cavities and fiber are in the vacuum state. Our goal is to deterministically realize the state swap between the two atomic systems:  $(\alpha_1|0, N\rangle_1 + \beta_1|1, N-1\rangle_1) \otimes (\alpha_2|0, N\rangle_2 + \beta_2|1, N-1\rangle_2) \rightarrow (\alpha_2|0, N\rangle_1 + \beta_2|1, N-1\rangle_1) \otimes (\alpha_1|0, N\rangle_2 + \beta_1|1, N-1\rangle_2)$ .

In the state swap, the three types of atomic states are involved: (1) $|0, N\rangle_1|0, N\rangle_2$ ; (2) $|1, N-1\rangle_1|0, N\rangle_2$ , and  $|0, N\rangle_1|1, N-1\rangle_2$ ; (3) $|1, N-1\rangle_1|1, N-1\rangle_2$ , which belong to subspaces with zero-, one- and two- excitation numbers, respectively. Since the Hamiltonian (5) conserves the total excitation number, Eq. (7) can be solved in each of the subspaces, respectively. When non photons are initially in both the cavities and fiber, the state  $|0, N\rangle_1|0, N\rangle_2 \otimes |000\rangle_f$  is unchanged. For the initial state  $(\beta_1\alpha_2|1, N-1\rangle_1|0, N\rangle_2 + \beta_2\alpha_1|0, N\rangle_1|1, N-1\rangle_2) \otimes |000\rangle_f$ , Eq. (7) is solved in the subspace spanned by the basis vectors (8). The two-excitation subspace is spanned by the basis vectors

$$|\phi_{n_1 n_f n_2}^{m_1 m_2}\rangle = |m_1, N-m_1\rangle_1 |m_2, N-m_2\rangle_2 \otimes |n_1 n_f n_2\rangle_f, \quad (18)$$

with the conditions  $0 \leq n_1, n_f, n_2, m_1, m_2 \leq 2$  and  $n_1 + n_f + n_2 + m_1 + m_2 = 2$ . In this subspace, the Dicke states  $|\varphi_{000}^{20}\rangle$  and  $|\varphi_{000}^{02}\rangle$  in which two atoms in the same cavity are simultaneously excited are involved. Here, we assume that the “dipole blockade” effect takes place, which was proposed by Lukin et al. [22] and observed in the recent experiments[23, 24, 25, 26]. This effect can highly depress the transition from single- to double excitation Dicke states. For the initial state  $|1, N-1\rangle_1|1, N-1\rangle_2 \otimes |000\rangle_f$ , we solve Eq. (7) in the subspace spanned by the basis vectors (18) with neglecting the double excitation Dicke states. On combining the results obtained from the zero-, single- and two-excitation subspaces, we can find the state  $|\Psi(t)\rangle$  of the entire system at time  $t$ .

If  $\alpha_i = \sin \theta_i$  and  $\beta_i = \cos \theta_i$ , the target state  $|\Psi_s\rangle$  is  $(\sin \theta_2|0, N\rangle_1 + \cos \theta_2|1, N-1\rangle_1) \otimes$

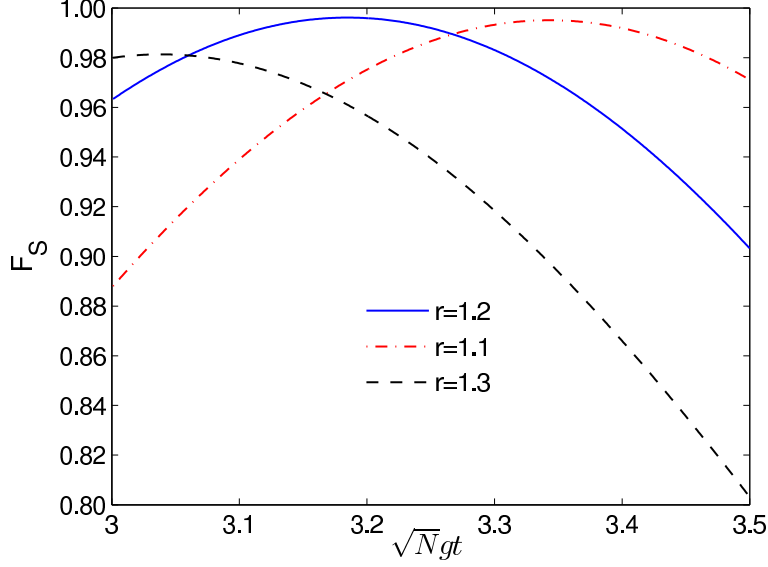


FIG. 3. The average fidelity of the swap gate as a function of  $\sqrt{N}gt$ .

$(\sin \theta_1 |0, N\rangle_2 + \cos \theta_1 |1, N-1\rangle_2) \otimes |000\rangle_f$ . The average fidelity of the swap gate is defined as

$$F_S = \frac{1}{4\pi^2} \int_0^{2\pi} d\theta_1 \int_0^{2\pi} d\theta_2 |\langle \Psi_s | \Psi(t) \rangle|^2. \quad (19)$$

In Fig. 3, the average fidelity is plotted as a function of  $\sqrt{N}gt$  for various values of the parameter  $r$ . It is observed that a highly reliable swap gate with the fidelity larger than 0.995 can be deterministically achieved at  $\sqrt{N}gt \simeq 3.2$  around  $r \simeq 1.2$ . Since the operation time of the swap gate is proportional to  $1/\sqrt{N}$ , the swap gate can be greatly speeded up when the number of atoms is large. In Fig. 3, one may also observe that the maximum of the fidelity is relatively stable with respect to the dimensionless time  $\sqrt{N}gt$  and the variation of the coupling constants.

## V. QUANTUM ENTANGLING GATE

In this section, we investigate to create the entangled states :  $(|1, N-1\rangle_1 |0, N\rangle_2 \pm |0, N\rangle_1 |1, N-1\rangle_2)/\sqrt{2}$ .

In the Schrödinger picture, the Hamiltonian (5) has the form

$$H = \omega(a_1^\dagger a_1 + a_2^\dagger a_2 + b^\dagger b + J_1^z + J_2^z) + H_{AF} + H_f, \quad (20)$$

where  $\omega$  is frequency of the transition between the excited and ground states of the two-level

atom, and  $J_j^z = \sum_{i=1}^N \sigma_i^z(j)$  with  $\sigma_i^z(j) = (|e_i\rangle\langle e_i| - |g_i\rangle\langle g_i|)/2$  for atom  $i$  in cavity  $j$ . Here, it is assumed that the interaction between the atoms and the cavity field, and the coupling between the cavity and fiber fields are on resonance. By use of the canonical transformations [20]

$$\begin{aligned} a_1 &= \frac{1}{2}(c_+ + c_- + \sqrt{2}c), \\ a_2 &= \frac{1}{2}(c_+ + c_- - \sqrt{2}c), \\ b &= \frac{1}{\sqrt{2}}(c_+ - c_-), \end{aligned} \quad (21)$$

three normal bosonic modes  $c$  and  $c_{\mp}$  are introduced. In terms of these new bosonic operators, the Hamiltonian (20) can be expressed as

$$\begin{aligned} H &= \frac{1}{2} \left[ g_1 J_1^+ (c_+ + c_- + \sqrt{2}c) + g_2 J_2^+ (c_+ + c_- - \sqrt{2}c) + \text{h.c.} \right] \\ &\quad + \omega(c^\dagger c + J_1^z + J_2^z) + (\omega + \sqrt{2}\nu)c_+ c_+^\dagger + (\omega - \sqrt{2}\nu)c_- c_-^\dagger. \end{aligned} \quad (22)$$

It is seen that frequencies of the normal mode  $c$  and  $c_{\mp}$  are  $\omega$  and  $\omega \mp \sqrt{2}\nu$ , respectively. Therefore, the mode  $c$  resonantly interacts with the atoms but the modes  $c_{\mp}$  non-resonantly interact with the atoms. For  $\nu \gg \sqrt{N}|g_j|$ , excitations of the nonresonant modes can be highly suppressed. In this case, the modes  $c_{\mp}$  can be safely neglected. In this way, the system reduces to two qubits resonantly coupled through a single-mode of the cavity field, and the Hamiltonian (22) in the interaction picture becomes

$$H = \frac{1}{\sqrt{2}} \left( g_1 J_1^- c^\dagger - g_2 J_2^- c^\dagger + \text{h.c.} \right). \quad (23)$$

Suppose that the atoms are in the state  $|1, N-1\rangle_1 |0, N\rangle_2$ , and the mode  $c$  is in the vacuum state at the initial time. From (23), the system at the later time is restricted to the subspace spanned by the basis vectors

$$\begin{aligned} |\phi_1\rangle &= |0\rangle_c |0, N\rangle_1 |1, N-1\rangle_2, \\ |\phi_2\rangle &= |0\rangle_c |1, N-1\rangle_1 |0, N\rangle_2, \\ |\phi_3\rangle &= |1\rangle_c |0, N\rangle_1 |0, N\rangle_2, \end{aligned} \quad (24)$$

where  $|0\rangle_c$  and  $|1\rangle_c$  are number states of the normal modes  $c$  with zero and one photon, respectively. Using the same method as in section III, one can show that at time  $t$  the

system evolves in the state

$$|\Psi(t)\rangle = \frac{g_1^2 + \cos(\sqrt{N(g_1^2 + g_2^2)/2} t) g_2^2}{g_1^2 + g_2^2} |\phi_1\rangle + \frac{g_1 g_2 - \cos(\sqrt{N(g_1^2 + g_2^2)/2} t) g_1 g_2}{g_1^2 + g_2^2} |\phi_2\rangle + i \frac{g_1 \sin(\sqrt{N(g_1^2 + g_2^2)/2} t)}{\sqrt{g_1^2 + g_2^2}} |\phi_3\rangle. \quad (25)$$

If requiring that the amplitude of  $|\phi_3\rangle$  vanishes and the absolute values of the amplitudes of  $|\phi_{1,2}\rangle$  in (25) are equal, we obtain the results:

**(a)** if  $g_2 = (1 + \sqrt{2})g_1$  and  $\sqrt{N}g_1 t = \pi/\sqrt{2 + \sqrt{2}}$ , the field comes back to the vacuum state and the atoms are in the entangled state  $|\psi_{E1}\rangle = (|1, N-1\rangle_1 |0, N\rangle_2 + |0, N\rangle_1 |1, N-1\rangle_2)/\sqrt{2}$ ;

**(b)** if  $g_2 = (-1 + \sqrt{2})g_1$  and  $\sqrt{N}g_1 t = \pi/\sqrt{2 - \sqrt{2}}$ , the field comes back to the vacuum state and the atoms are in the entangled state  $|\psi_{E2}\rangle = (|1, N-1\rangle_1 |0, N\rangle_2 - |0, N\rangle_1 |1, N-1\rangle_2)/\sqrt{2}$ .

If  $N_1 \neq N_2$ , we also find that the entangled states can be generated if either  $\sqrt{N_2}g_2 = (1 + \sqrt{2})\sqrt{N_1}g_1$  or  $\sqrt{N_2}g_2 = (-1 + \sqrt{2})\sqrt{N_1}g_1$  is fulfilled.

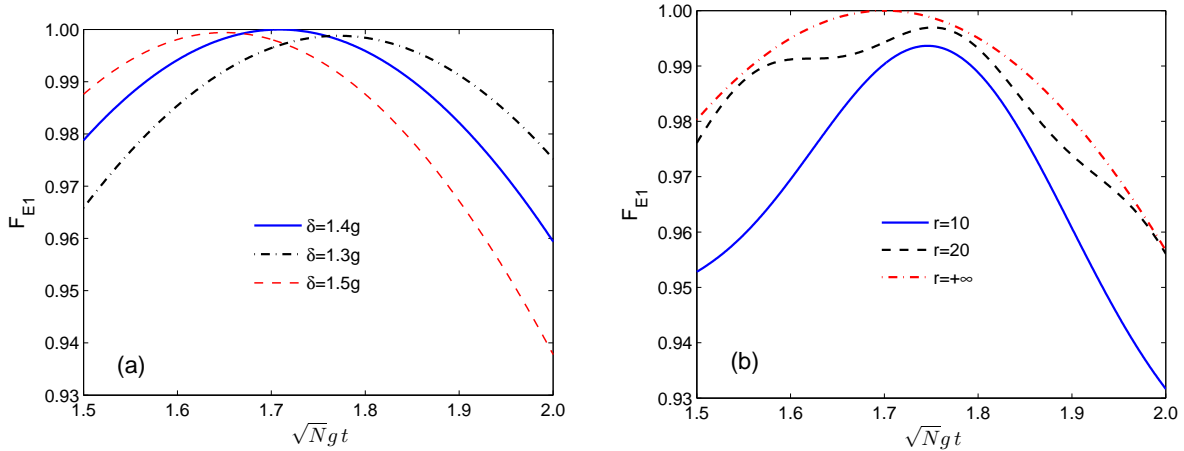


FIG. 4. Fidelity of the entangling gate versus  $\sqrt{N}gt$ . (a)  $r = \infty$ ; (b)  $\delta = \sqrt{2}g$ .

In practical situations, the ratio of the coupling constants required for realizing the entangling gate may not be satisfied exactly. In order to see the effects of the imperfections in the coupling constants, we define fidelity of the entangling gate:  $F_{Ei} = |\langle \Psi(t) | \psi_{Ei} \rangle|^2$ . In Fig. 4(a), setting  $g_1 = g$  and  $\delta = g_2 - g_1$ , we plot the fidelity as a function of the dimensionless

time  $\sqrt{N}gt$  for different values of the parameter  $\delta$ . It is seen that the fidelity is remarkably robust to the deviation of the coupling constants from the values for the perfect entangling gate.

In order to check in which regime the non resonant normal modes can be safely neglected, we directly solve Eq. (7) in the subspace spanned by the basis vectors (8). In the calculation, we suppose that the atoms are initially in  $|1, N-1\rangle_1|0, N\rangle_2$  and all the field modes are in the vacuum state. In Fig. 4(b), the fidelity is plotted for different values of the parameter  $r$ . It is observed that the maximum of the fidelity can be larger than 0.99 if  $r$  is beyond 20.

Similar to the swap gate, the operation time of the entangling gate is also proportional to  $1/\sqrt{N}$ . Therefore, the entangling gate can be greatly speeded up as the number of atoms increases.

## VI. CONTROLLED-Z GATE

In this section, we investigate how to realize the controlled-Z gate between the two atomic systems:  $(|0, N\rangle_1 + |1, N-1\rangle_1) \otimes (|0, N\rangle_2 + |1, N-1\rangle_2)/2 \rightarrow (|0, N\rangle_1|0, N\rangle_2 + |0, N\rangle_1|1, N-1\rangle_2 + |1, N-1\rangle_1|0, N\rangle_2 - |1, N-1\rangle_1|1, N-1\rangle_2)/2$  [27]. A controlled-Z gate is important in building quantum computers since a CNOT gate [28] can be constructed from one controlled-Z gate and two Hadamard gates [27].

As in the proceeding section, we assume that the limit  $\nu \gg \sqrt{N}|g_j|$  is valid. In the controlled-Z gate operation, when the resonant c-mode is initially in the vacuum state, the three types of atom states are involved: (1) $|0, N\rangle_1|0, N\rangle_2$ ; (2) $|1, N-1\rangle_1|0, N\rangle_2$  and  $|0, N\rangle_1|1, N-1\rangle_2$ ; (3) $|1, N-1\rangle_1|1, N-1\rangle_2$ , which belong to subspaces with the zero-, single- and two- excitation numbers, respectively. The zero subspace contains only one state:  $|0, N\rangle_1|0, N\rangle_2$ . The single-excitation subspace is spanned by the basis vectors (24).

The two-excitation subspace is spanned by the basis vectors

$$\begin{aligned}
|\phi_1\rangle &= |0\rangle_c |1, N_1 - 1\rangle_1 |1, N_2 - 1\rangle_2, \\
|\phi_2\rangle &= |1\rangle_c |0, N_1\rangle_1 |1, N_2 - 1\rangle_2, \\
|\phi_3\rangle &= |1\rangle_c |1, N_1 - 1\rangle_1 |0, N_2\rangle_2, \\
|\phi_4\rangle &= |2\rangle_c |0, N_1\rangle_1 |0, N_2\rangle_2, \\
|\phi_5\rangle &= |0\rangle_c |2, N_1 - 2\rangle_1 |0, N_2\rangle_2, \\
|\phi_6\rangle &= |0\rangle_c |0, N_1\rangle_1 |2, N_2 - 2\rangle_2.
\end{aligned} \tag{26}$$

In the last two vectors, two atoms in the same cavity are excited. Here, we assume that the "dipole blockade" effects [22] take place. Then, the double-excitation Dicke states can be neglected.

Since the total excitation number  $c^\dagger c + N_1 + N_2$  is conserved in the coherent evolution governed by the Hamiltonian (23), using the same method in section III, we solve the Schrödinger equation with the Hamiltonian (23) in the zero-, single- and two-excitation subspaces for the initial states  $|0, N\rangle_1 |0, N\rangle_2$ ,  $(|1, N - 1\rangle_1 |0, N\rangle_2 + |0, N\rangle_1 |1, N - 1\rangle_2)/\sqrt{2}$ , and  $|1, N - 1\rangle_1 |1, N - 1\rangle_2$ , respectively. On combining the results obtained from the subspaces, we can find the state  $|\Psi(t)\rangle$  of the entire system at time  $t$  with the initial condition  $|\Psi(0)\rangle = |0\rangle_c \otimes (|0, N\rangle_1 + |1, N - 1\rangle_1) \otimes (|0, N\rangle_2 + |1, N - 1\rangle_2)/2$ . For the controlled-Z gate, the target state is  $|\Psi_Z\rangle = |0\rangle_c \otimes (|0, N\rangle_1 |0, N\rangle_2 + |0, N\rangle_1 |1, N - 1\rangle_2 + |1, N - 1\rangle_1 |0, N\rangle_2 - |1, N - 1\rangle_1 |1, N - 1\rangle_2)/2$ . Then, the fidelity of the controlled-Z gate is defined as  $F_Z = |\langle \Psi_Z | \Psi(t) \rangle|^2$ .

In the calculation, as section in V, let's set  $g_1 = g$  and introduce the parameter  $\delta = g_2 - g_1$ . The controlled-Z gate can be realized by properly choosing the parameter  $\delta$ . As shown in Fig. 5, for  $\delta \simeq 0.07g$ , the controlled-Z gate with the fidelity larger than 0.999 is achieved at  $\sqrt{N}gt \simeq 54.3$ . If  $\delta = 0.35g$ , the controlled-Z gate with the fidelity bigger than 0.999 reaches at  $\sqrt{N}gt \simeq 10.80$ . If  $\delta = 1.20$ , the controlled-Z gate with the fidelity larger than 0.99 is realized at  $\sqrt{N}gt \simeq 3.4$ . In the calculation, it is noticed that the controlled-Z gate is speeded up as the parameter  $\delta$  increases. The sensitivity of the fidelity to the difference between the atom-field couplings has also been checked. With comparing Fig. 6(a) to Fig. 6(b), one may find that the larger  $\delta$  is and the more insensitive the fidelity to the coupling difference is. In the non-resonant and one-atom case [20], it was also pointed out that the larger  $\delta$  is and the less the operation time of the controlled-Z gate is. However, the fidelity and the stability of the quantum gate greatly decrease as the parameter  $\delta$  increases. In the

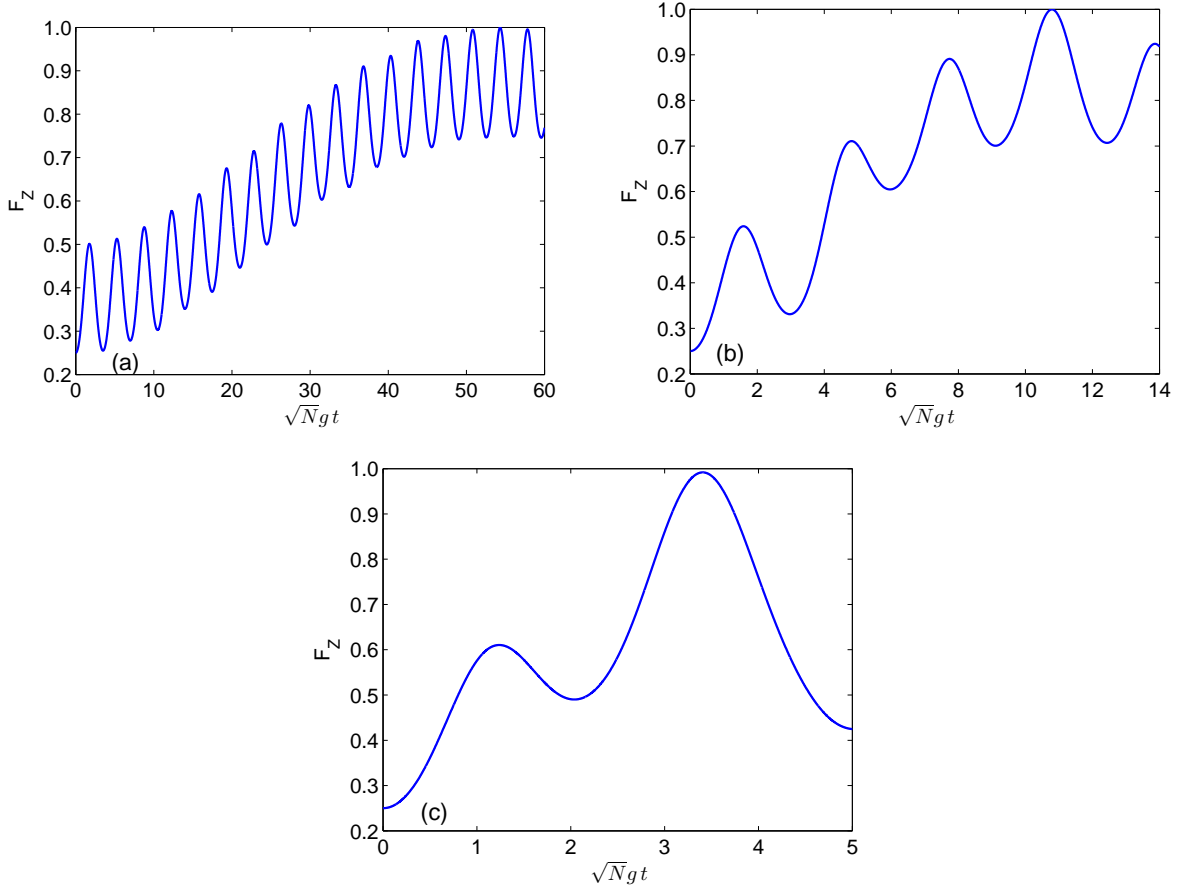


FIG. 5. Fidelity of the controlled-Z gate as a function of  $\sqrt{N}gt$  with  $\delta =$  (a)  $0.07g$ ; (b)  $0.35g$ ; (c)  $1.2g$ .

resonant and multiatom case under consideration, as the parameter  $\delta$  increases, the stability of the quantum gate is highly enhanced but meanwhile the fidelity decreases only from 0.999 to 0.99. In Fig. 6(c), the results obtained by directly solving the Schrödinger equation (7) with  $\delta = 0.35g$  are shown. It is noticed that the off-resonant modes can be safely neglected in implementing the controlled-Z gate when  $r = \nu/(\sqrt{N}g) > 20$ .

In the present scheme, all the atoms interact resonantly with the cavity fields. We find that the resonant interaction can greatly speed up the operation of the controlled-Z gate. For example, if  $\delta = 1.2g$  and  $N = 1$ , the operation time needed to implement the controlled-Z gate is only  $1/8$  of the time needed in the nonresonant case that was considered in [20]. Meanwhile, in the multiatom case, the operation time of the controlled-Z gate is proportional to  $1/\sqrt{N}$ . Therefore, we expect that the controlled-Z gate based on the multi atoms and the resonant interaction can run much faster than on the single atom and the nonresonant

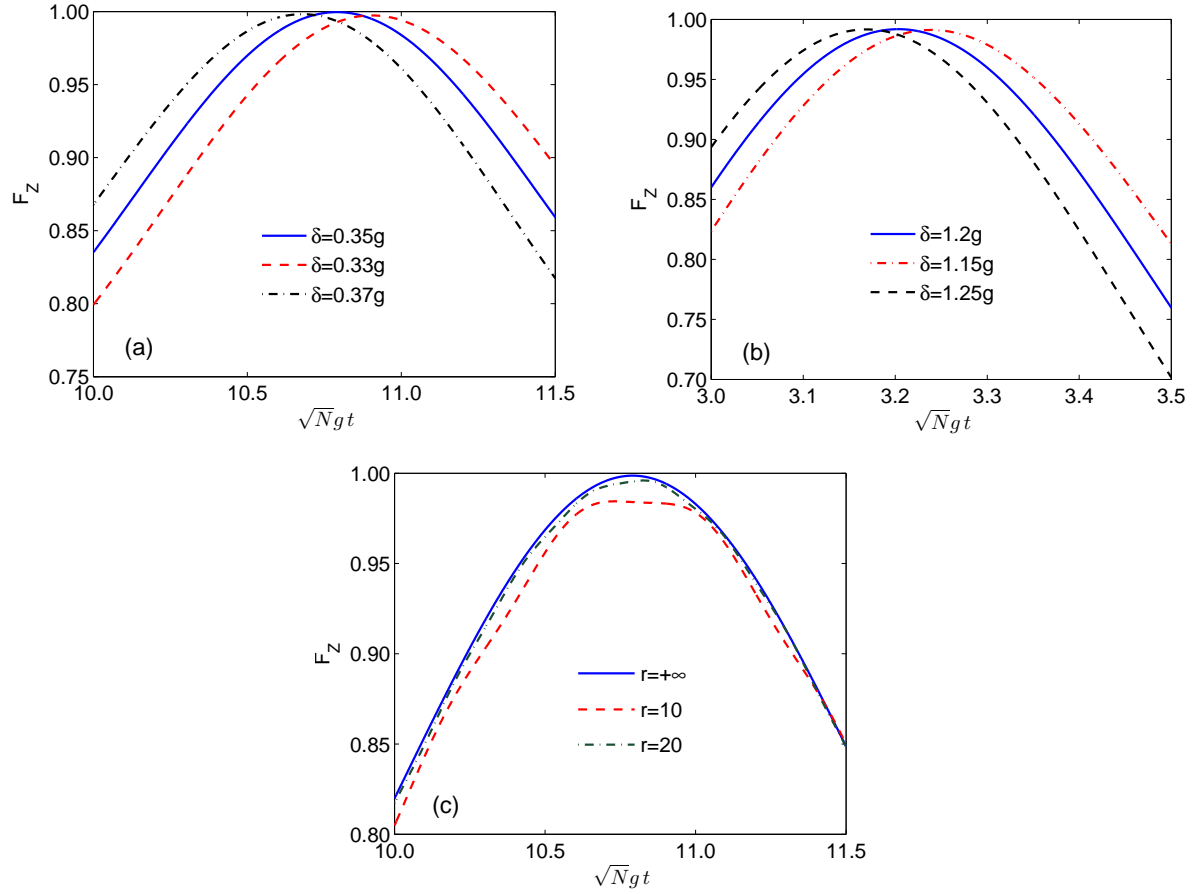


FIG. 6. Fidelity of the controlled-Z gate as a function of the dimensionless time  $\sqrt{N}gt$ .

interaction. In this way, the influence of dissipations such as spontaneous emission and cavity and fiber losses on the operation of the controlled-Z gate may be greatly diminished.

## VII. EFFECTS OF SPONTANEOUS EMISSION AND PHOTON LEAKAGE

In this section, we investigate the influence of atomic spontaneous emission and photon leakage out of the cavities and fiber on the quantum state transfer, and the swap, entangling and controlled-Z gates which have been discussed in the previous sections.

In the present calculation, we assume that the atoms interact collectively with the privileged local cavity modes but individually with other modes of the electromagnetic field. This scheme may be realized by properly arranging the spatial distribution of atoms in cavity. For example, the spatial distribution shape of atoms may be made so narrow along the axial direction of the cavity that all the atoms see the same field and collectively interact with the

cavity field but so wide along the transversal direction that all the atoms can individually interact with all modes of the electromagnetic field except the cavity one. We will later discuss this point in detail and show this arrangement can be realized with present cavity and trap techniques. Based on the consideration, the master equation of motion for the density matrix of the entire system may be written as

$$\begin{aligned} \dot{\rho} = & -i[H, \rho] + \gamma \sum_{j=1}^2 L[a_j]\rho + \beta L[b]\rho \\ & + \kappa \sum_{j=1}^2 \sum_{i=1}^N \left[ 2\sigma_i^-(j)\rho\sigma_i^+(j) - \sigma_i^+(j)\sigma_i^-(j)\rho - \rho\sigma_i^-(j)\sigma_i^+(j) \right], \end{aligned} \quad (27)$$

where  $L[o]\rho = 2o\rho o^\dagger - o^\dagger o\rho - \rho o^\dagger o$ , and  $\kappa$ ,  $\gamma$  and  $\beta$  are rates, respectively, for spontaneous emission of the atoms, photon leakage out of the cavity and fiber. For simplicity, we assume the rates equal for both the cavities and the mean number of thermal photons in both the cavities and fiber is zero.

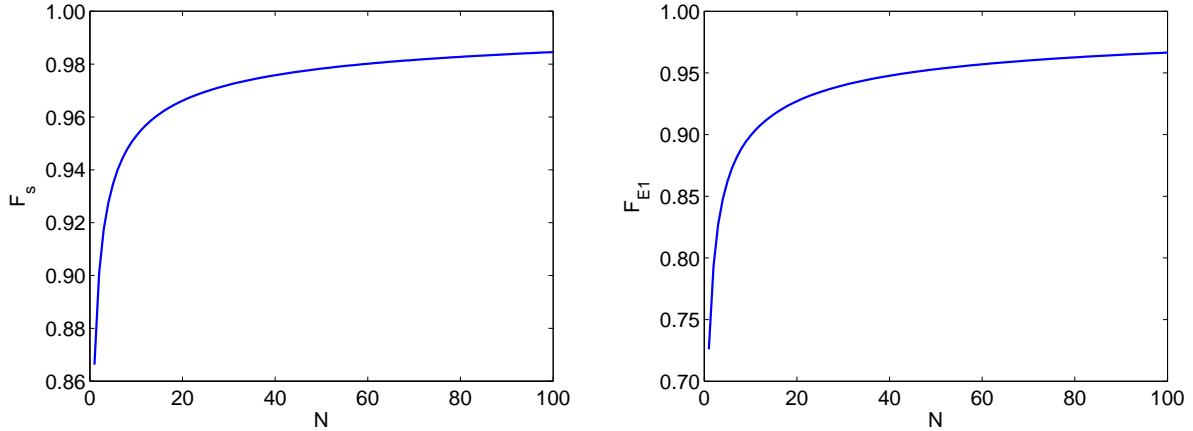


FIG. 7. Fidelity of (a) the state transfer and (b) the entangling gate as a function of the number of atoms.

At first, let's consider the state transfer:  $(|0, N\rangle_1 + |1, N-1\rangle_1)/\sqrt{2} \otimes |0, N\rangle_2 \rightarrow |0, N\rangle_1 \otimes (|0, N\rangle_2 + |1, N-1\rangle_2)/\sqrt{2}$ . In this case, the master equation (27) is numerically solved in the space spanned by the basis vectors (8) and  $|000\rangle_f |0, N\rangle_1 |0, N\rangle_2$ . In the calculation,  $g_1 = g_2 = g$  and  $\kappa = \gamma = \beta = 0.1g$  are chosen. For the state transmission under consideration, the target state is  $|\Psi_s\rangle = |000\rangle_f \otimes |0, N\rangle_1 \otimes (|0, N\rangle_2 + |1, N-1\rangle_2)/\sqrt{2}$ . Fidelity of the state transfer is defined as  $F_s(t) = \langle \Psi_s | \rho(t) | \Psi_s \rangle$ . In Fig. 7(a), the maximum of the fidelity is plotted against number of the atoms trapped in each of the cavities. It is observed that

the nearly perfect state transmission with the fidelity beyond 0.96 can be realized when the number of atoms is larger than 20.

For the swap gate  $(\sin \theta_1 |0, N\rangle_1 + \cos \theta_1 |1, N-1\rangle_1) \otimes (\sin \theta_2 |0, N\rangle_2 + \cos \theta_2 |1, N-1\rangle_2) \rightarrow (\sin \theta_2 |0, N\rangle_1 + \cos \theta_2 |1, N-1\rangle_1) \otimes (\sin \theta_1 |0, N\rangle_2 + \cos \theta_1 |1, N-1\rangle_2)$ , we assume that the "dipole blockade" effects [22] take place. This allows to ignore the double-excitation Dicke states in the calculation. The master equation (27) is numerically solved in the space spanned by the basis vectors (8), (18) and  $|000\rangle_f |0, N\rangle_1 |0, N\rangle_2$ . In the calculation,  $g_1 = g_2 = g$  and  $\kappa = \gamma = \beta = 0.1g$  are chosen. The average fidelity of the swap gate is defined as

$$F_S = \frac{1}{4\pi^2} \int_0^{2\pi} d\theta_1 \int_0^{2\pi} d\theta_2 |\langle \Psi_s | \rho(t) | \Psi_s \rangle|, \quad (28)$$

where  $|\Psi_s\rangle = (\sin \theta_2 |0, N\rangle_1 + \cos \theta_2 |1, N-1\rangle_1) \otimes (\sin \theta_1 |0, N\rangle_2 + \cos \theta_1 |1, N-1\rangle_2) \otimes |000\rangle_f$ . For  $N = 100$ , we obtain the maximal fidelity 0.958. For  $N = 10^4$ , we obtain the maximal fidelity 0.992. In the single-atom scheme [20], one has to take  $\kappa = \gamma = \beta = 0.001g$  for obtaining the same maximum values of the fidelity. Therefore, in the multiatom scheme, the relatively reliable swap gate can be realized even if the strength of the coherent interaction between the atoms and the cavity field is not much larger than the rates of spontaneous emission and photon leakage.

As shown in section IV, when  $\nu \gg \sqrt{N}g$ , we may introduce the resonant mode  $c$ . Since the fiber mode is not involved in the mode  $c$  according to the transformations (21), the entangling and controlled-Z gates are unaffected by fiber losses in this limitation. In this case, therefore, the master equation of motion for the atoms and the resonant mode  $c$  can be written as

$$\dot{\rho} = -i[H, \rho] + \gamma L[c]\rho + \kappa \sum_{j=1}^2 \sum_{i=1}^N \left[ 2\sigma_i^-(j)\rho\sigma_i^+(j) - \sigma_i^+(j)\sigma_i^-(j)\rho - \rho\sigma_i^-(j)\sigma_i^+(j) \right], \quad (29)$$

For the entangling gate, Eq. (29) is solved in the space spanned by the basis vectors (24) and  $|0\rangle_c |0, N\rangle_1 |0, N\rangle_2$  with the initial state  $|0\rangle_c |1, N-1\rangle_1 |0, N\rangle_2$ . In the calculation,  $g_1 = g_2, \kappa = \gamma = 0.1g$  and  $\nu = 50\sqrt{N}g$  are chosen. For concretion, we consider the target state  $|\psi_{E1}\rangle = |0\rangle_c [|1, N-1\rangle_1 |0, N\rangle_2 + |0, N\rangle_1 |1, N-1\rangle_2] / \sqrt{2}$ . Fidelity of the entangling gate is defined as  $F_{E1} = \langle \psi_{E1} | \rho(t) | \psi_{E1} \rangle$ . In Fig. 7(b), the maximum of the fidelity is plotted against the number of atoms. It is observed that the entangling gate with the fidelity bigger than 0.95 is realized when  $N \geq 50$ .

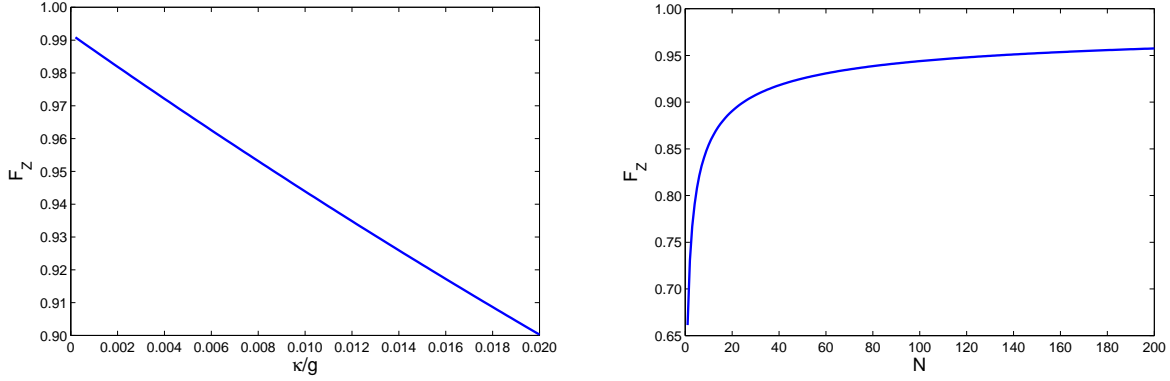


FIG. 8. (a) Fidelity of the controlled-Z versus the decay rate  $\kappa = \gamma$ . (b) Fidelity of the controlled-Z gate as a function of the atomic number.

For the controlled-Z gate, Eq. (29) is solved in the space spanned by the basis vectors

$$|\psi_{n_c m_1 m_2}\rangle = |n_c\rangle_c |m_1, N - m_1\rangle_1 |m_2, N - m_2\rangle_2 \quad (30)$$

$$\text{with } 0 \leq n_c, m_1, m_2 \leq \mathcal{N}, \quad n_c + m_1 + m_2 = \mathcal{N}, \quad \text{and } 0 \leq m_1, m_2 \leq 1,$$

where  $\mathcal{N} (= 0, 1, 2)$  is the total excitation number. In the calculation, we assume that at the initial time the entire system is in the state  $|0\rangle_c \otimes (|0, N\rangle_1 + |1, N - 1\rangle_1) \otimes (|0, N\rangle_2 + |1, N - 1\rangle_2)/2$  and take  $g_1 = g, \delta = g_2 - g_1 = 1.2g$ , and  $\gamma = \kappa$ . The target state is  $|\Psi_Z\rangle = |0\rangle_c \otimes (|0, N\rangle_1 |0, N\rangle_2 + |0, N\rangle_1 |1, N - 1\rangle_2 + |1, N - 1\rangle_1 |0, N\rangle_2 - |1, N - 1\rangle_1 |1, N - 1\rangle_2)/2$ . Fidelity of the controlled-Z gate is defined as  $F_Z(t) = \langle \Psi_Z | \rho(t) | \Psi_Z \rangle$ . In Fig. 8(a), the maximum of the fidelity is shown against the decay rate  $\kappa$  when  $N = 1$ . It is observed that the controlled-Z gate with the fidelity larger than 0.96 is realized for  $\kappa = \gamma \simeq 0.006g$ . For the controlled-Z gate with the same fidelity, the condition  $\kappa = \gamma \simeq 0.0001g$  is required in the nonresonant case that was considered in [20]. Therefore, the resonant scheme under consideration can highly depress the effects of spontaneous emission and photon leakage out of the cavity. Now let's consider the multiatom case. In this case, we take  $\kappa = \gamma = 0.1g$  and other parameters same as above. In Fig. 8(b), the maximum of the fidelity is shown as the number of atoms. It is seen that even for such a large decay rate the controlled-Z gate with the fidelity bigger than 0.95 is achieved when  $N \geq 150$ .

In the recent experiment [29], (34MHz, 2.6MHz and 4.1MHz) for  $(g, \kappa, \gamma)/2\pi$  are achieved. Even more strong-coupling ( $\kappa/g \geq 165$ ) [30, 31] and ultrahigh-Q ( $\simeq 10^8$ ) microcavity[30] have been predicted and proved experimentally. Therefore, the condition  $g \sim 10\gamma$  that is required in the present scheme can be satisfied by use of the developed techniques. As for

the fiber coupling to the cavities, a perfect fiber-cavity coupling (with efficiency larger than 99.9%) can be realized by fiber-taper coupling to high-Q silica microspheres [32]. On the other hand, it is also possible to locate atoms in an optical cavity with the spatial precision  $\lambda/10$  [33]. Therefore, we should believe that it is feasible with present techniques to realize the quantum processes under consideration in this paper.

## VIII. SUMMARY

We investigate how to deterministically implement quantum state transfer, and swap, entangling and controlled-Z gates between two subsystems consisting of two-level atoms trapped in single-mode cavities spatially separated and connected by an optical fiber. If the atoms collectively and resonantly interact with the local fields, we find that a perfect quantum state transfer can be realized if the ratio of the coupling constant between the atoms and the cavity field to the coupling constant between the fiber and cavity modes satisfies the established condition. If the event for two atoms to be simultaneously excited in the same cavity is depressed by the "dipole blockade" effect, it is shown that a nearly perfect swap gate can be realized. When the coupling between the fiber and cavity modes is much stronger than the coupling between the atoms and the cavity field, the entire system can be approximated as two qubits resonantly coupling to a harmonic oscillator. In this limitation, the nearly perfect entangling and controlled-Z gates can be realized. It is also noticed that the quantum computation processes under investigation are much robust against the variation of the coupling constants. We find that the operation time of the quantum state transfer and the quantum logic gates is proportional to  $1/\sqrt{N}$  where  $N$  is number of the atoms in each of the cavities. Therefore, the quantum computation processes can be greatly speeded up when the number of atoms becomes large. This effect is useful for depressing the influence of unavoidable decoherence processes such as spontaneous emission and photon leakage. By numerically solving the master equation of motion for the entire system, we investigate the influence of spontaneous emission of the atoms and photon leakage out the cavities and fiber on the quantum computation processes. In the calculation, we assume that the atoms collectively interact with the privileged cavity modes but individually decay to other modes of the electromagnetic field. We find that when the number of atoms is large the quantum computation processes can be accomplished with high fidelity even if rates of

the dissipations are large around the order of one-tenth of the coherent coupling strength between the atoms and local cavity fields.

The above conclusions are based on the following assumptions: (1) there does not exist direct interaction between the atoms when all the atoms are in the ground state; (2) the atoms collectively interact with the cavity mode; (3) the dipole blockade effect takes place; (4) the atomic spontaneous emission is individual. We now investigate if these conditions can be fulfilled in current experiments. For a concrete purpose, let us take alkali atomic levels  $7s_{1/2}$  and  $np_{3/2}$  ( $n \sim 50$ ) as the ground state  $|g\rangle$  and the excited state  $|e\rangle$  in the present discussion, respectively [26]. Since the atom resonantly interacts with the cavity field, corresponding the atomic transition, the wavelength of the cavity field ranges from 700 to 800 nm. Suppose that the cavity field has the spatial distribution  $E(r, z) = E_0 e^{-\frac{r^2}{W^2}} \cos(kz)$  where  $W$  is the waist width and  $k$  is the wave vector of the cavity field [34]. The coupling strength between the cavity field and the atom is given by  $g(r, z) = g_0 e^{-\frac{r^2}{W^2}} \cos(kz)$ . Suppose that all the atoms are trapped in a shaped-flat-disk trap of transverse radius  $\delta r$  and axis-thickness  $\delta z$  in the cavity. This flat-disk trap with the radius  $\delta r = 2.3 \mu\text{m}$  and the thickness  $\delta z = 33 \text{ nm}$  has been realized in experiments [29]. The no interaction condition requires  $d \gg r_g$ , where  $d$  is the average distance between two atoms and  $r_g$  is the radius of the atom in the ground state. Since  $\delta r \gg \delta z$ , we may approximately consider that the atoms have a surface distribution in the trap. In this way, the average distance may be estimated by  $d = \sqrt{\pi(\delta r)^2/N}$ , where  $N$  is the number of atoms in the trap. Consider an alkali atom with the valence electron in  $ns$  state. The orbit radius of the valence electron is approximately given by  $n^2 a_0$ , where  $a_0$  is the Bohr radius. With current experiment parameters [29], for  $7s_{1/2}$  of Cs atom, we have  $r_g \approx 2.6 \text{ nm}$  and  $d \approx 4.1N^{-1/2} \mu\text{m}$ . Therefore, the no direct interaction condition can be satisfied very well when  $N < 200$ . The collective interaction condition requires that the variation of the coupling strength in the trap must be very small, that is,  $\delta g/g_0 \ll 1$ , or  $k\delta z \ll 1$  and  $\delta r \ll W$ . In the current experiment [29],  $k\delta z \approx 0.26$  and  $\delta r \approx 0.1W$ . The spatial variation in the trap results in the change of the coupling strength  $\delta g/g_0 < 10^{-2}$ . Thus, all the atoms in the trap have the nearly same coupling strength and then collectively interact with the cavity field. We now check the dipole blockade condition. The dipole blockade mechanism assumes that a strong interaction such as either the van der Waals interaction [23, 24, 25] or dipole-dipole interaction [26] takes place when two atoms in an alkali atomic ensemble are simultaneously excited into Rydberg states. This strong

interaction can make the Rydberg level shifts so large that all the transitions into states with more than a single excitation are blocked [22]. This excitation blockade phenomenon has been demonstrated in several experiments [23, 24, 25, 26]. In order to guarantee the occurrence of the dipole-blockade mechanism, the condition  $d \sim r_e$  is required, where  $r_e$  is the radius of the atom in the excited state. For the Rydberg level  $50p_{3/2}$  [26],  $r_e \approx 0.13 \mu\text{m}$ . For the Rydberg level  $80p_{3/2}$  [23, 24, 25],  $r_e \approx 0.34 \mu\text{m}$ . For  $N = 100$ ,  $d \sim 0.4 \mu\text{m}$ . Thus, the dipole-blockade mechanism can take place when  $N > 100$ . From the above discussion, we see that the no interaction condition has to be traded off to the dipole blockade condition. In this way, the number of atoms in the trap is limited around 200 with the current experiment parameters. Therefore, with the current cavity and trap techniques [33, 35], the present multiatom scheme may speed up the operation of the logical gates by 10 times. As regards spontaneous emission, for  $N = 100$ , from the above parameters, we have  $kd \sim 3$ , that is, along the transverse direction, the average distance of atoms is larger than the reduced wavelength of the cavity field. On the other hand, only one atom is excited if the dipole blockade effect takes place. Therefore, in the present scheme, we can consider that the excited atoms individually couple to all transverse modes of the electromagnetic field [22, 36, 37]. Here, the key point is that the atoms are trapped in the flat-disk-trap. The trap is so narrow along the cavity axis and slowly varying in the transverse direction that the atoms collectively interact with the cavity field but so wide in the transverse direction that the atoms individually decay. In summary, according to parameters in current experiments, the essential assumptions employed in the present scheme are reasonable and realistic. The multiatom quantum state transfer and quantum logic gates could be realized with current optical cavity and atomic trap techniques.

## Acknowledgments

Zhang-qi Yin thanks Hong-rong Li, Peng Peng and Ai-ping Fang for valuable discussions. This work was supported by the Natural Science Foundation of China (Grant Nos. 10674106,

- 
- [1] P. W. Shor, in *Proceedings, 35<sup>th</sup> Annual Symposium on Foundations of Computer Science* (IEEE Press, Los Almitos, CA, 1994), p. 124.
  - [2] L. K. Grover, *Phys. Rev. Lett.* **79**, 325 (1997).
  - [3] J. I. Cirac and P. Zoller, *Nature* **404**, 579 (2000).
  - [4] J. I. Cirac, A. K. Ekert, S. F. Huelga, and C. Macchiavello, *Phys. Rev. A* **59**, 4249 (1999).
  - [5] M. Paternostro, M. S. Kim, and G. M. Palma, *J. Mod. Opt.* **50**, 2075 (2003).
  - [6] D. P. DiVincenzo, *Phys. Rev. A* **51**, 1015 (1995).
  - [7] A. Barenco, C. H. Bennett, R. Cleve, D. P. DiVincenzo, N. Margolus, P. Shor, T. Sleator, J. A. Smolin, and H. Weinfurter, *Phys. Rev. A* **52**, 3457 (1995).
  - [8] L. M. Duan and H. J. Kimble, *Phys. Rev. Lett.* **92**, 127902 (2004).
  - [9] Y. L. Lim, A. Beige, and L. C. Kwek, *Phys. Rev. Lett.* **95**, 030505 (2005).
  - [10] S. D. Barrett and P. Kok, *Phys. Rev. A* **71**, 060310(R) (2005).
  - [11] J. Cho and H. W. Lee, *Phys. Rev. Lett.* **95**, 160501 (2005).
  - [12] Y. F. Xiao, X. M. Lin, J. Gao, Y. Yang, Z. F. Han, and G. C. Guo, *Phys. Rev. A* **70**, 042314 (2004).
  - [13] J. I. Cirac, P. Zoller, H. J. Kimble, and H. Mabuchi, *Phys. Rev. Lett.* **78**, 3221 (1997).
  - [14] T. Pellizzari, *Phys. Rev. Lett.* **79**, 5242 (1997).
  - [15] S. J. van Enk, H. J. Kimble, J. I. Cirac, and P. Zoller, *Phys. Rev. A* **59**, 2659 (1999).
  - [16] S. Clark, A. Peng, M. Gu, and S. Parkins, *Phys. Rev. Lett.* **91**, 177901 (2003).
  - [17] D. E. Browne, M. B. Plenio, and S. F. Huelga, *Phys. Rev. Lett.* **91**, 067901 (2003).
  - [18] L. M. Duan and H. J. Kimble, *Phys. Rev. Lett.* **90**, 253601 (2003).
  - [19] S. Mancini and S. Bose, *Phys. Rev. A* **70**, 022307 (2005).
  - [20] A. Serafini, S. Mancini, and S. Bose, *Phys. Rev. Lett.* **96**, 010503 (2006).
  - [21] F. L. Li, X. S. Li, D. L. Lin, and T. F. George, *Phys. Rev. A* **41**, 2712 (1990).
  - [22] M. D. Lukin, M. Fleischhauer, R. Cote, L. M. Duan, D. Jaksch, J. I. Cirac, and P. Zoller, *Phys. Rev. Lett.* **87**, 037901 (2001).
  - [23] D. Tong, S. M. Farooqi, J. Stanojevic, S. Krishnan, Y. P. Zhang, R. Côté, E. E. Eyler, and P. L. Gould, *Phys. Rev. Lett.* **93**, 063001 (2004).

- [24] K. Singer, M. Reetz-Lamour, T. Amthor, L. G. Marcassa, and M. Weidemüller, Phys. Rev. Lett. **93**, 163001 (2004).
- [25] T. C. Liebisch, A. Reinhard, P. R. Berman, and G. Raithel, Phys. Rev. Lett. **95**, 253002 (2005).
- [26] Thibault Vogt *et al.*, Phys. Rev. Lett. **97**, 083003 (2006).
- [27] M. A. Nielsen and I. L. Chuang, *Quantum Computation and Quantum Information* (Cambridge University Press, Cambridge, United Kingdom, 2000).
- [28] A. Barenco, D. Deutsch, and A. Ekert, Phys. Rev. Lett. **74**, 4083 (1995).
- [29] A. Boca, R. Miller, K. M. Birnbaum, A. D. Boozer, J. McKeever, and H. J. Kimble, Phys. Rev. Lett. **93**, 233603 (2004).
- [30] S. M. Spillane, T. J. Kippenberg, K. J. Vahala, K. W. Goh, E. Wilcut, and H. J. Kimble, Phys. Rev. A **71**, 013817 (2005).
- [31] M. Trupke *et al.* (2005), quant-ph/0506234.
- [32] S. M. Spillane, T. J. Kippenberg, O. J. Painter, and K. J. Vahala, Phys. Rev. Lett. **91**, 043902 (2003).
- [33] P. Maunz, T. Puppe, I. Schuster, N. Syassen, P. W. H. Pinkse, and G. Rempe, Phys. Rev. Lett. **94**, 033002 (2005).
- [34] C. J. Hood *et al.*, Science **287**, 1447 (2000).
- [35] Stefan Nußmann *et al.*, Nature Physics **1**, 122 (2005).
- [36] Z. Ficek and R. Tanas, Physics Reports **372**, 369 (2002).
- [37] L. M. Duan, M. D. Lukin, J. I. Cirac, and P. Zoller, Nature **414**, 413 (2001).